

## CONTROL OF INSULATION CONDITION OF SMART GRIDS BY MEANS OF CONTINUOUS PD MONITORING

Fernando GARNACHO  
LCOE-FFII – Spain  
fgarnacho@lcoe.etsii.upm.es

Miguel Ángel SÁNCHEZ-URÁN  
UPM-Spain  
miguelangel.sanchezuran@upm.es

Javier ORTEGO  
UPM-Spain  
javier.ortego@upm.es

Fernando ÁLVAREZ  
UPM – Spain  
fernando.alvarez@upm.es

Alberto GONZÁLEZ  
Gas Natural Fenosa-Spain  
agonzalezsan@gasnatural.com

### ABSTRACT

*This paper presents the monitoring architecture and experience gained in a pilot distribution grid designed for continuous control of insulation condition of the grid by means of PD measurements. Powerful data processing tools are used for the discrimination of PD pulses from background noise, for locating different PD sources, for clustering PD sources and for identification of the defect associated to each PD source.*

### INTRODUCTION

Service continuity of electric supply is a priority for Smart Grids. Consequently, the knowledge of insulation condition in Smart Grids should be considered as a relevant performance.

Partial Discharges measurements [1] and [2] have been the most accepted technique in the world to evaluate the insulation condition of high voltage equipment (power cables, cable joints, cable terminations, voltage and current transformers, power transformers, gas insulated switchgear apparatus, etc.). It is known, that incipient insulation defects provoke small electrical partial discharges (PD) in different kind of insulation media (XLPE, SF<sub>6</sub>, epoxy resins, etc.). When the insulation is degraded, PD pulses increase in rate or/and amplitude up to breakdown. An uncontrolled breakdown in high voltage cables provokes critical and dangerous conditions that can compromise grid integrity.

The insulation condition of the electrical grids can be determined by means of “off line” PD tests [3]. Mobile high voltage generators, such as VLF generators, Damping Alternating Current generators (DAC) or Resonant Generators (ACRL or ACRF) allow performing on site tests with PD measurements [4] and [5]. However, in the latest years, the progressing of unconventional PD measurements [6] and the huge advance in data processing [7] has allowed continuous PD monitoring for analyzing the insulation condition of high voltage electrical grids. This technology recently implemented in transmission grids can be also adapted to the particular requirements of the electrical distribution grids.

### ARCHITECTURE FOR PD MONITORING IN DISTRIBUTION SMART GRIDS

Continuous PD monitoring in distribution Smart Grids requires measuring autonomous systems (MAS) distributed along the cable system to be monitored, that must be placed in strategic substations. A Control Analysis System (CAS) installed in a substation centralizes the data sent by the MAS units installed along the cable system to be monitored. The data can be sent by optical fiber, by GPRS messages or by PLC. Each CAS analyzes received data to evaluate the insulation condition of the cable system. Automatic alarms and personalized analysis are combined to detect incipient defects and to avoid unexpected failures (see figure 2).

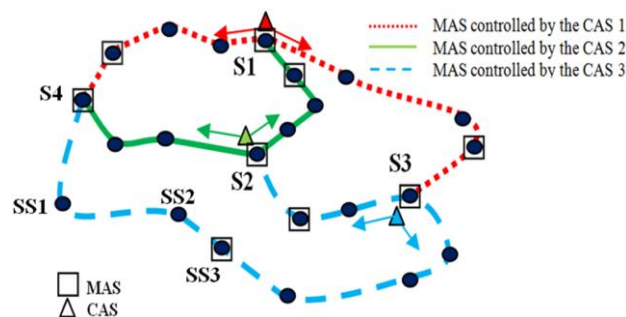


Figure 1. a) Architecture for PD Monitoring in Smart Grids

Figure 1 shows three CAS units installed in three substations (S1, S2 and S3) for PD monitoring of a grid of three MV lines. An appropriate number of MAS units are installed in strategic MV/LV substations along cable system. The place where each MAS must be installed is chosen in order to assure sensitivity enough for PD detection caused by a defect in any cable section of the cable to be monitored.

MAS units are designed to PD measuring in the frequency range between 0.5 MHz and 15 MHz in order to be sure that the amplitude of PD signal that travels along cable system is not strongly attenuated and can be detected, at least, by two PD sensors. The PD monitoring system allows using capacitors coupled to h.v. conductor or High Frequency

Transformers Current (HFCT) installed at the sheath cable when it is connected to earth. An additional UHF sensor can be installed at the both ends of each cable system in order to analyze whether any PD signal detected at the cable end is caused in the cable termination itself or away from the cable termination. A digital recorder of 14 bits of vertical resolution and 100 Msamples/s is used to acquire PD signals. Signals acquired by UHF sensors require a signal converter to be matched to the input of the PD instrument. Finally, a set of powerful processing tools are used to PD diagnosis.

The criterion to decide where MAS units must be placed is by means of analyzing PD attenuation along the cable system for the measuring frequencies. The approach consists of injecting bursts of sinusoidal signals of different oscillation frequencies in the range of interest frequencies (e.g. from 1 MHz to 10 MHz). The signals are injected through the cable sheath installed in substation by means a HFCT or through the cable conductor by means of a coupling capacitor.

PD sensors installed in each substation (MV/LV) of the cable system to be monitorized allow evaluating of amplitude attenuation of sinusoidal signals injected. Figure 2 shows bursts of sinusoidal signals of 7 MHz injected through the cable sheath from the substation S4, that corresponds with the cable end. The figure 2 also shows signals measured by PD sensors installed at the three consecutive substations (MV/LV) placed at 378 m (SS1), 750 m (SS2) and 1080 m (SS3) from the S4 substation.

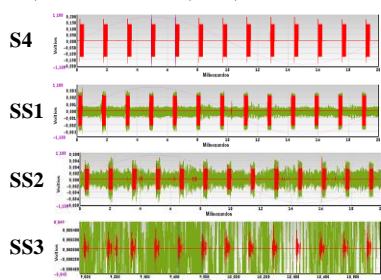


**Figure 2.** Bursts sinusoidal signals of 7 MHz acquired by PD sensors placed in the injection substation S4 and in three consecutive substations: SS1, SS2 and SS3.

The signal attenuation in three consecutive substations when a sinusoidal signal of a specific frequency is injected through cable sheath is shown in figure 3-a. The attenuation at the SS1 substation is higher than at SS2 substation in spite of SS2 substation is emplaced more far than SS1 from the injection point (substation S4). Consequently, at the SS1 substation there is an over-attenuation. The over-attenuation at the SS1 substation is ratified for frequencies smaller than 4 MHz when sinusoidal signal is injected through cable conductor (see figure 3-b). In addition, a resonance mode appears around of 4 MHz at the SS1 and SS2 substations.

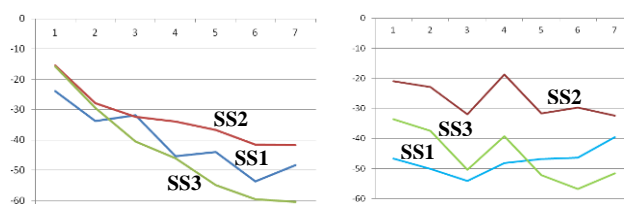


**Figure 3.** Amplitude-frequency attenuation for sinusoidal signal: a) injected through the cable sheath, b) injected through the cable conductor.

**DIAGNOSIS TOOLS**

Powerful data processing tools are used for the discrimination of PD pulses from background noise, for locating different PD sources and for PD clustering in order to identify a defect or the cause associated to each PD source by means of the a neural network for recognition of phase-resolved PD patterns.

**Noise suppression**

A filtering tool on the basis of wavelet transform improved allows discriminating PD signals from noise signals. Electronic pulses caused by power electronics connected to electrical grid have a similar transient behavior as PD pulses, for this reason they are not removed by the wavelet filtering but by means of the 3D waveform clustering tool. In practice, many PD signals hidden behind background noise originated by broadcasting stations, TV stations or white noise can be discriminated using the improved wavelet filtering (figure 4).

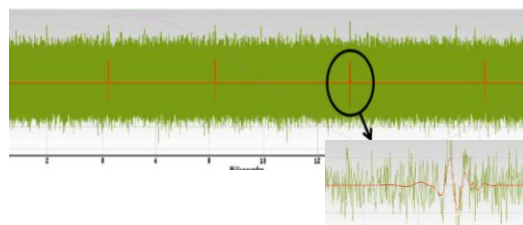


**Figure 4.** Wavelet filtering: PD pulses mixed with white noise.

An example of PD measurements of a cable system using the improved wavelet filtering is shown in figure 5. The most significant difference of the improved wavelet filtering used in comparison with other conventional digital filtering is the inexistence of a noise threshold.

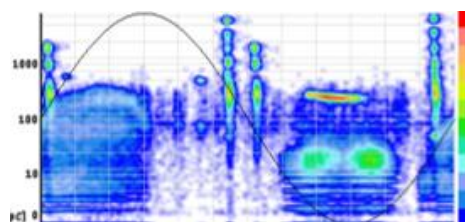


**Figure 5.** Phase resolved PD pattern applying wavelet filtering.

**PD mapping tool**

When a PD source appears in a cable system, two PD pulses travel towards opposite senses along cable system. In general, each PD pulse arrives to each PD measuring unit placed at the cable end, in a different instant. The subtraction between both arrival times allows determining the site where the PD source is originated. The main difference of this PD mapping approach in comparison with other approaches is the determination of the arrival time of the PD pulse, that is identified by the starting instant of PD pulse instead of the instant associated to the maximum peak value of the PD pulse that is used by traditional methods. This is possible thanks to the powerful of the filtering tool. Figure 7 shows an example of the map of PD sources along cable system under monitoring. In this example three different locations of PD sources are shown.

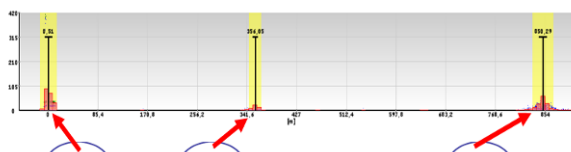


**Figure 6.** Example of clustering for PD location: a) PD pulses in the left end of the cable system, b) PD pulses at 356 m from left cable end and c) PD pulses at the right end of the cable system.

**3D- waveform clustering tool**

Each PD pulse  $i$ -th filtered by the improved wavelet filter is modeled by the  $i_i(t)$  function composed by a sine function  $g_i(t)$  modulated by an enveloping function  $h_i(t)$ .

$$i_i(t) = g_i(t) \cdot h_i(t) \tag{2}$$

with:

$$g_i(t) = A_i \cdot \sin(\omega_i \cdot t - \psi_i) \tag{3}$$

$$h_i(t) = \frac{1}{e^{\alpha_i \cdot (t-t_{0i})} + e^{-\beta_i \cdot (t-t_{0i})}} \tag{4}$$

Where:

- $t$ : time variable,
- $g_i(t)$ : the sine function associated with the  $i$ <sup>th</sup> PD pulse, with amplitude  $A_i$ , oscillation frequency  $f_i = [\omega_i / 2\pi]$  and displacement from the instant  $t = 0$   $\psi_i$  radians,
- $h_i(t)$ : function that modulates the sine function.
- $\alpha_i$  and  $\beta_i$ : shape parameters of  $h_i(t)$ .
- $t_{0i}$ : temporary displacement of  $h_i(t)$ .

Figure 7 shows the application of the 3D ( $\alpha$ ,  $\beta$  and  $f$ ) waveform clustering tool that allows separate four different DPs patterns: three of which do not involve an insulation defect (power electronics pulses IGBTs, corona DPs and a metallic element floating-ungrounded) and another PDs focus (DPs superficial pulses) associated with dirty on the

outer surface of the insulation of the termination, which will require cleaning maintenance.

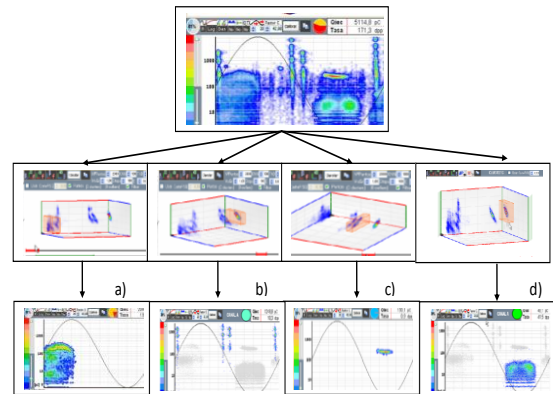


**Figure 7.** Example of 3D PD clustering: a) surface PD pulses, b) power electronics, c) corona effect, d) floating metal element.

**NOISE SUPPRESSION CAPABILITY TEST**

A test to determine noise suppression capability was performed to compare capabilities of different PD sensors and different technologies of commercial PD instruments. A signal function generator is used to generate random signal (Noise Generator-NG-) that is superimposed as an interference signal on the PD signals to be measured. A PD source of 400 pC provoked by a cavity defect in a XLPE insulation of a cable is used. The output of the NG was amplified (A) if necessary in to order to hide PD signals.

Two different PD sensors were tested: a) coupling capacitor with a measuring impedance ( $C_k + Z_m$ ) and b) High Frequency Current Transformer (HFCT). Three different kinds of PD measuring approaches were compared: i) unconventional PD measurements applying the improved wavelet filtering (BB) ii) unconventional PD measurements applying a selective frequency band for PD measurements ( $7\text{MHz} \pm 1\text{MHz}$ ) (MI) and iii) a standard PD instrument according to IEC 60270 (S).

Figure 8 shows the testing setup for noise suppression test when is compared the measuring approaches MI and BB, using HFCT sensors in both cases.

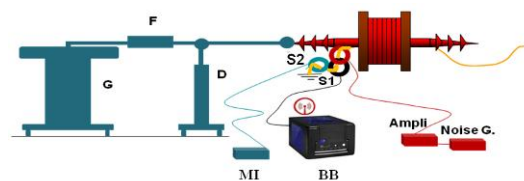


**Figure 8.** Testing setup for noise suppression test. G: H.V. generator. F: Filter, D: voltage divider. MI and BB: PD measuring instruments

The best results were obtained when the coupling capacitor

( $C_k+Z_m$ ) and the BB approach were used. Table 1 shows the comparison between the unconventional PD measurement approach (BB) and the standard PD measurement approach (S) using the two different sensors. Results show that using the standard approach (S), PD signals cannot be detected if noise level achieves the amplitude of PD signals, while unconventional approach using wavelet filtering (BB) can remove noise interference from PD signals in spite of the noise level is 10 times greater to PD amplitude (see table 1). Although noise influence affects stronger to HFCT sensor than  $C_k+Z_m$  sensor, no intrusive sensor (HFCT) is usually preferred, because its sensitivity is good enough to detect internal insulation defects.

	$C_k+Z_m$		HFCT	
	Noise level: 5 pC	Noise level: 400 pC	Noise level: 5 pC	Noise level: 400 pC
BB Instrument	400pC 100%	90%	70%	60%
IEC 60270				
	Noise level: 800 pC	Noise level: 4000 pC	Noise level: 800 pC	Noise level: 4000 pC
BB Instrument	70%	25%	35%	No detection

Table 1. PD source 400 pC + White Noise

### EXPERIENCE OF PD MONITORING IN MV

PD evolution during two months of a new MV cable system of 4.1 km with nine accessories per phase is displayed in figure 9. In total, six PD sources appeared since the cable was energized. The two PD sources that appeared in the phase R are shown on the right side of figure 9. Immediately after the cable was commissioned DP were detected in a cable end of phase R and 17 days later of commissioning DP signals appeared in the joint B. These two PD sources were analyzed. The first one, located at the cable termination, was associated to corona effect and the other to a cavity defect (see figure 9).

The evolution of the PD rate and the PD amplitude are shown in figure 10. Both evolutions associated to corona effect were maintained quite constant. However the PD amplitude of the cavity defect decreased progressively during approximately 1.5 months from inception level to a stabilization level, around 10% of the initial amplitude. At the same time, during this time period, the PD rate increased from 8 pulses per period (20 ms) up to 50 pulses per period.

After three months operating the defective joint was changed. Clear assembling mistakes and degradation signs were found in the defective joint. After joint replacement no PD signals were detected by the monitoring system.

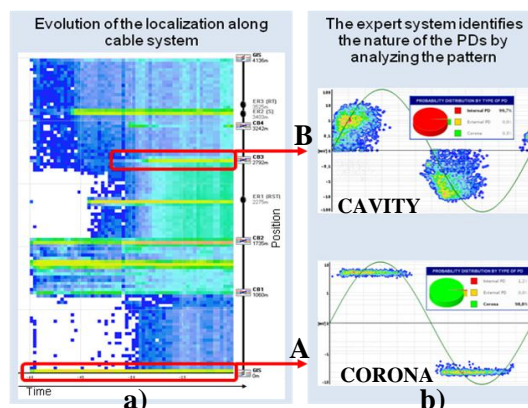


Figure 9. PD evolution: a) time-cable length. b) Patterns: A) Corona at a cable end B) Cavity defect.

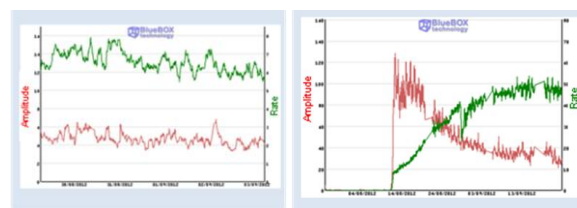


Figure 10. PD rate and PD amplitude evolution: a) Corona at a cable end b) Cavity defect in a cable joint.

### Acknowledgments

Special acknowledgments for Gas Natural Fenosa for actively promoting research projects on partial discharges in HV and MV networks and AENA for your confidence in insulation diagnosis of their MV grids.

### REFERENCES

- [1] IEC 60270 standard, 2000. "High-voltage test techniques - Partial discharge measurements".
- [2] E. Lemke et al., 2008 "Guide for electrical Partial Discharge Measurements in compliance to IEC 60270". CIGRE Brochure 366, WG D1.33.
- [3] IEC 60060-3 standard "High-voltage test techniques-Part 3-Definitions and requirements for on-site testing
- [4] R. Pietsch et al, "High-Voltage On-Site Testing with Partial Discharge Measurement", CIGRE Brochure 502 W G D1.33.
- [5] IEEE Guide for Partial Discharge Testing of Shielded Power Cable Systems in a Field Environment IEEE Std 400.3-2006
- [6] E. Gulski et al, 2010 "Testing on site Guidelines for Unconventional Partial Discharge Measurements" CIGRE Brochure 444. WG D1.33
- [7] F. Garnacho et al, 2010 "Partial discharge monitoring system for high voltage cables". CIGRE, Paris August 2010, paper B1 306.